Efficient targeted DNA editing and replacement in Chlamydomonas reinhardtii using Cpf1 ribonucleoproteins and single-stranded DNA

Classification

BIOLOGICAL SCIENCES, Plant Biology

Title

Efficient targeted DNA editing and replacement in *Chlamydomonas reinhardtii* using Cpf1 ribonucleoproteins and single-stranded DNA

Short title

Efficient DNA replacement in *Chlamydomonas*

Author Affiliation

Aron Ferenczi, Douglas Pyott, Andromachi Xipnitou and Attila Molnar

University of Edinburgh, Institute of Molecular Plant Sciences, Mayfield Road, Edinburgh, EH9 3BF, United Kingdom

Corresponding author

Attila Molnar, email: attila.molnar@ed.ac.uk, Tel: 0044 131 6505335

Keywords

Chlamydomonas reinhardtii, CRISPR/Cpf1, RNP, editing, ssODN

Author contributions

AM conceived and guided the study. AF and AM designed the experiments. AF performed algal and *in vitro* experiments, AX performed Western blots, DP and AM performed *in planta* experiments. AF and AM analyzed the data and wrote the manuscript with input from all authors.

Abstract

The green alga *Chlamydomonas reinhardtii* is an invaluable reference organism to research fields including algal, plant and ciliary biology. Accordingly, decades-long standing inefficiencies in targeted nuclear gene editing broadly hinder *Chlamydomonas* research. Here we report that single-step co-delivery of CRISPR/Cpf1 ribonucleoproteins with single-stranded DNA repair templates results in precise and targeted DNA replacement with up to ~10% efficiency in *C. reinhardtii*. We demonstrate its use in transgene- and selection-free generation of sequence-specific mutations and epitope tagging at an endogenous locus. Since the direct delivery of gene editing reagents bypasses the use of transgenes, this method is potentially applicable to a wider range of species without the need to develop methods for stable transformation.

Significance Statement

Our findings demonstrate a new method of efficient, targeted genome editing in *Chlamydomonas reinhardtii*. We demonstrate a novel approach to bypass inefficient gene targeting via homologous recombination (HR) and achieve homology-directed DNA replacement in *C. reinhardtii*. In addition, we report CRISPR/Cpf1-mediated DNA editing efficiencies being boosted 500-fold through use of single-stranded oligodeoxynucleotides (ssODNs) as repair templates. It remains to be determined whether Cpf1-induced staggered DNA cleavage enhances ssODN-mediated gene editing in a wider range of species and whether the underlying repair pathway(s) responsible is more broadly conserved.

\body

Introduction

The model green microalga *Chlamydomonas reinhardtii* is an invaluable model organism at the interface of algal, plant and ciliary biology (1, 2). For decades, *C. reinhardtii* has fueled research on photosynthetic gene function (3), and is an indispensable reference for studying the carbon concentrating mechanism (4, 5), ciliary function and composition (6-8), lipid metabolism and prospects of biofuel production (9-11), carotenoid biosynthesis (12) and nutrient starvation responses (13-15). *C. reinhardtii* is remarkably tractable owing to its short generation time (8-10h), haploid genotype, sequenced genome (16, 17), simple transformation methods (18-21) and plethora of resources including the Chlamydomonas Resource Center (University of Minnesota) and The Chlamydomonas Sourcebook (22).

Despite its auspicious features, nuclear gene targeting in *C. reinhardtii* through homologous recombination (HR)-mediated plasmid integration occurs at prohibitively low levels (18, 19, 23-28). This necessitates the positive selection of mutants through cointegration of antibiotic resistance markers. The recent use of single-stranded oligodeoxynucleotides (ssODNs) has reduced non-target integration, but has left gene targeting extremely inefficient (29-32). Previous efforts to use targeting endonucleases, including Zinc Finger Nucleases (ZFNs) and Clustered Regularly Interspaced Short Palindromic Repeat (CRISPR)-associated protein 9 (Cas9), have not resolved these shortcomings in gene targeting efficiency (33-36).

RNA-programmable CRISPR endonucleases induce targeted, double-stranded DNA breaks, triggering cellular DNA repair pathways. Of these pathways, non-homologous end-joining (NHEJ) results in random insertions and deletions (indels) at the target site (37, 38), while HR allows homology-directed, precise editing using DNA repair templates. NHEJ-mediated gene editing efficiencies in *C. reinhardtii* using Cas9 are low, ranging from 10^{-8} to 1% (35, 36) and so require phenotype-based selection of mutants. In addition, CRISPR-mediated editing in *C. reinhardtii* is presently limited to NHEJ-mediated indel formation due to an apparent insufficiency in the nuclear HR pathway to carry out homology-mediated editing (35, 36) .

Here, we report that transgene-free transfection into *C. reinhardtii* of pre-assembled CRISPR/Cpf1 ribonucleoproteins, an orthologue of Cas9, can induce NHEJ-mediated indels with 0.02% efficiency, broadly matching that of Cas9 (32, 36). More importantly, co-transfection of Cpf1 with single-stranded oligodeoxynucleotides (ssODNs) acting as DNA repair templates results in precise, targeted DNA replacement at frequencies up to 10%. This enables phenotype-independent identification of mutants edited with nucleotide-level precision at nuclear loci predisposed to Cpf1-mediated cleavage.

Results

Our goal was to devise an efficient Cpf1-mediated genome-editing platform for *C. reinhardtii*, member of a basally diverged clade (*Chlorophyta*) of the plant kingdom (39). We first tested the activity of two Cpf1 orthologues *in planta* by *Agrobacterium*-mediated transient expression in *Nicotiana benthamiana*. Since Cas9 activity *in planta* is correlated with activity in mammalian cells (40), we assayed the activity of *Acidaminococcus* Cpf1 (AsCpf1) and *Lachnospiraceae* Cpf1 (LbCpf1), the then known most active Cpf1 orthologs in mammalian cells (41, 42). By expressing AsCpf1, LbCpf1, Cas9 and corresponding guide RNAs in *N. benthamiana* we found the activity of LbCpf1 broadly matched Cas9, while AsCpf1 activity was barely detectable through a T7 cleavage assay (Fig. 1*A*). We concluded that LbCpf1 is more active than AsCpf1 *in planta*, in agreement with other recent studies (43-46), and therefore proceeded with LbCpf1 to edit *C. reinhardtii*.

To monitor LbCpf1-mediated genome editing in *Chlamydomonas*, we targeted *FK506-binding protein 12* (*FKB12*, Cre13.g586300) for knock-out. FKB12 mediates the interaction between the antibiotic rapamycin and the cell cycle regulator Target Of Rapamycin (TOR), which leads to cell death. Consequently, *FKB12* loss-of-function mutation results in high rapamycin tolerance (resistance), making it a suitable marker for positive selection in targeted mutagenesis (34, 47). We identified two LbCpf1 guide RNA (gRNA) protospacer adjacent motifs (PAMs, 5'-TTTN-3') within the second exon of *FKB12* and designed a gRNA for the one having no predicted off-target sites with Cas-OFFinder (48). We generated the gRNA by *in vitro* transcription and purified recombinant LbCpf1 protein from *E. coli*. To assess the activity of our CRISPR reagents, the target *FKB12* locus was PCR amplified and incubated with pre-assembled LbCpf1 and gRNA ribonucleoprotein (RNP) complexes *in vitro*. The complete *in vitro* cleavage of the target locus confirmed active RNP formation (Fig. 1*B*).

To test the efficacy of LbCpf1 *in vivo*, we delivered the *FKB12*-targeting RNPs into *C. reinhardtii* cells (cc-1883, *cw15*) via electroporation and spread cells onto solid growth media containing 10 µM rapamycin (36). Cell viability, required to determine the proportion of rapamycin resistant cells, was estimated from serial dilution of cells that had undergone identical electroporation treatment but without gRNA and were grown on media containing no rapamycin (Fig. S1).

Delivery of RNPs produced ~0.02% rapamycin resistant cells. Through sequencing, we confirmed 13 out of 16 rapamycin resistant colonies having mutations at the LbCpf1 cut site (Fig. 1*C*), equivalent to a mutagenesis efficiency of 0.016%. This underrepresents total mutagenesis efficiency as it only represented loss-of-function mutations. Colonies with no detectable *FKB12* mutations were most likely cells that escaped selection, as we never experienced total elimination of background cell growth using even 20mM rapamycin.

We next explored whether targeted DNA cleavage could be used to facilitate homology-mediated mutagenesis using DNA repair templates. We employed single-stranded oligodeoxynucleotide (ssODN) templates, which reportedly provide 100-fold lower levels of non-homologous integrations compared with double-stranded counterparts (29). Our ssODN was 118 nucleotides long, designed with homology arms extending 49 and 45 nucleotides upstream and downstream of the gRNA target site, respectively. It harbored replacement of the target site with a foreign sequence of equal length with stop codons inserted in all three reading frames. We tested the single-step co-delivery of RNPs together with ssODNs in either the sense or antisense orientation (Fig. 2*A*). To calculate editing efficiency, cells were serially diluted and each dilution was plated onto solid growth media with and without rapamycin to estimate numbers of mutant cells and viable cells, respectively. Surprisingly, co-delivery of RNPs and ssODN led to 22% and 18% rapamycin resistant cells using sense and antisense ssODNs, respectively (Fig. 2*B*). Sequencing of rapamycin resistant colonies confirmed template integration in most cases (n=27/32), though single-nucleotide indels and substitutions were scattered across the region of ssODN homology in half (n=14/27) of all sequenced mutants (Fig. *2C,* Fig. S2 and Fig. S3*A*). Two integration events resulted in duplication of the homology arms (Fig. S7). Importantly, scarless integration events represented 40% (n=13/32) and 46% (n=6/13) of rapamycin-resistant cells using sense and antisense ssODNs, respectively, which we regarded as being broadly equivalent. As a proportion of viable cells, scarless, homology-mediated editing was achieved in 8-9% efficiency, which represents a ~500-fold increase over non-ssODN-mediated knock-outs using RNPs alone. In control experiments using sense ssODNs without RNPs, resistant cells were rare ($2x10^{-3}$%; Fig. 2*B*), on a par with previously established protocols (29, 31).

To demonstrate the utility of ssODN-mediated gene editing in *Chlamydomonas*, we epitope tagged the endogenous *FKB12* in frame (Fig. 3*A*). We designed a sense ssODN as described above and replaced the gRNA target site with six tandem histidine codons followed by an in-frame stop codon. The stop codon allowed mutation efficiencies to be estimated from the frequency of rapamycin resistant cells as before (see Fig 2*B*). Co-delivery of RNPs and this ssODN yielded 29% rapamycin resistant colonies (Fig. 3*B*). Sequences from six such colonies suggested that around half carried scarless integrations (Fig. 3*C*). This high frequency (>10% of viable cells) raised the possibility of identifying colonies containing scarless DNA replacement without first selecting against wild-type cells. This approach could be used even when the phenotypic effects of a mutation might not be obvious or are unknown. To test this, thirteen randomly chosen colonies growing on non-selective medium (without rapamycin) were sequenced. One of these colonies carried the desired DNA replacement (representing 7% of viable cells), demonstrating viable selection- and phenotype-free identification of edited cells (Fig. 3*D*). Immunoblot analysis confirmed a detectable his-tagged protein

of the expected size in the identified mutants (Fig. 3*E*) and is one of the first demonstrations of epitope tagging at an endogenous locus in *C. reinhardtii* (32).

To transfer our method into a cell walled strain of *C. reinhardtii*, we attempted to edit *FKB12* in cell-walled strain cc-2931. The same electroporation conditions did not result in rapamycin resistance, even after treating cells with Maxx Efficiency Transformation Reagent (Fig. S4).

To explore the efficacy of LbCpf1 and ssODN-mediated editing at other nuclear loci, we targeted 3 additional genes in strain cc-1883: *CpFTSY* (Cre05.g241450), *CpSRP43* (Cre04.g231026) and *PHT7* (Cre16.g663600). CpFTSY and CpSRP43 are nuclear encoded components of the chloroplast signal recognition particle and are involved in assembly of the chlorophyll light-harvesting complexes (LHCs), also called antennae (49). Loss-of-function mutation at these loci results in truncated chlorophyll antennae leading to lower chlorophyll content and hence a bright-green phenotype (36, 49, 50). Phenotypic screening for bright-green colonies therefore allows determination of loss-of-function mutation efficiency. In contrast, PHT7 is a putative phosphate transporter in *C. reinhardtii* and was included to represent a locus with no known phenotype.

Interestingly, *in vitro* cleavage of *CpFTSY*, *CpSRP43* and *PHT7* occurred with varying efficacies (Fig. 4*A*). Editing at these loci was performed using ssODNs harboring the same target site replacement as before with in-frame stop codons. As expected, colonies with *CpFTSY* and *CpSRP43* mutations displayed a bright green phenotype (Fig. 4*B* and Fig. S6). Surprisingly, *PHT7* mutants elicited a growth disadvantage and could be identified through a small-colony phenotype (Fig. 4*B* and Fig. S5*A*). Hence targeted editing at *PHT7* was equally suitable for efficiency determination.

Targeted knock-out of *CpFTSY*, *CpSRP43* and *PHT7* occurred in 0.5% to 16% of cells, of which ssODN-mediated, scarless DNA editing occurred in 0.1% to 8% of cells (Fig. 4*C*, *D*, Fig. S5 and Fig. S6). Larger insertions were consistently a result of sequence duplications (Fig. S7). Together with editing at *FKB12*, ssODN-mediated, scarless targeted editing occurs with 0.1% to 10% efficiency, with overall knock-out efficiencies at a slightly higher 0.5% to 16%.

Discussion

Our work demonstrates that the use of CRISPR/LbCpf1 ribonucleoproteins (RNPs) and single-stranded oligodeoxynucleotides (ssODNs) as DNA repair templates can perform efficient, homology-directed editing in *C. reinhardtii*. At four nuclear loci, we show scarless editing to occur with efficiencies of 0.1% to 10%, while scarred editing occurs with up to 16%.

Nuclear homologous sequence replacement in *C. reinhardtii* has been reported as inefficient and taken as evidence for low activity of the nuclear HR repair pathways (27). Our findings of gene

targeting efficiencies being much higher than previously reported suggests an alternative homology-directed mechanism distinct from HR is invoked through ssODN-mediated repair. This might also be more broadly conserved within plants and eukaryotes. Indeed, in human cells, ssODN-mediated repair has been shown to be independent of canonical HR components BRCA2 and RAD51 (51, 52). In addition, the staggered cuts produced by Cpf1 may efficiently predispose to homology-mediated ligation of ssODNs at the cut site, potentially more so than at Cas9-mediated blunt cuts. Furthermore, high-throughput nuclear transgenesis of *C. reinhardtii* suggests sequence-specific endonucleases extensively fragment transgenes prior to integration (53). This compounds the difficulties in performing precise, HR-mediated nuclear gene targeting. Use of single-stranded DNA may bypass endonuclease recognition, although local ssODN fragment duplications still occur presumably through stochasticity of the thermodynamic DNA annealing process (Fig S6).

Despite the ~500-fold enhancement of editing through supplementation of RNPs with ssODNs, we observed two orders of magnitude variability in nuclear editing efficiencies at four nuclear loci. These results partly reflect a lack of tools to predict Cpf1-mediated DNA cleavage efficiency (54), which are more abundant for Cas9 (55-59). *In vivo* Cpf1 cleavage efficiencies are distinct from Cas9 and markedly vary even within tens of bases of DNA (36, 60), which suggests a significant sequence-specific component to cleavage efficiency. We therefore take the lower range of our demonstrated editing efficiencies (0.1% - 1%) to reflect inefficient gRNA design. Curiously, DNA cleavage *in vitro* did not correlate with results *in vivo* (Fig 4*A*, *D*). This counterintuitive finding suggests to us that *in vitro* cleavage is not suitable to infer *in vivo* results. To increase editing efficiencies, lowering the number of electroporated cells, lowering the volume of electroporated cells and increasing Cpf1 concentration might be employed. In addition, testing multiple targets per locus can empirically reveal efficient gRNAs (36, 57). We also conclude that editing of cell-walled *C. reinhardtii* strains will continue to require autolysin treatment to degrade cell walls prior to transfection (19). Pulsed, square-wave electroporation has also been optimized for cell-walled strains and may offer viable means of transfection (32, 61).

Delivery of RNPs bypasses the need to develop a system for genetic transformation of the target species, including transgene optimization and selection of transgenic cells. The high potential efficiency of editing may also remove the need to select for mutants by phenotype. The approach could therefore be applicable to a wider range of green algal species, promoting their use in industry and basic research.

Materials and Methods

Generation of Cpf1, Cas9 and GFP-targeting guide RNA constructs. Plasmid vectors containing human-codon optimized Cpf1 from *Acidamonococcus* sp. BV3L6 (AsCpf1) and *Lachnospiraceae* bacterium ND2006 (LbCpf1) were a gift from Feng Zhang (Addgene plasmids #69982 and #69988, respectively). The Cpf1 coding sequence and C-terminal nuclear localization signal were PCR amplified to include 5' SpeI and 3' BsrGI sites and a C-terminal HIS tag (Table S1). PCR fragments were cloned into plant transformation binary vector pK7FWG2 as SpeI-BsrGI fragments. GFP-targeting Cpf1 guide RNA sequences were added downstream of the U6 promoter by PCR using pEN-Chimera (62) as template DNA (Table S1). Resultant PCR products were cloned as SmaI-EcoRV fragments into vector pK7FWG2. The GFP-targeting Cas9 guide RNA sequence was annealed using two single-stranded oligonucleotides and ligated into BbsI-linearized pEN-Chimera (Table S1). The customized RNA chimera was then transferred into Cas9-expressing plant transformation binary vector pDe-CAS9 by a single site Gateway LR reaction (Invitrogen) as previously described (62).

***Nicotiana benthamiana* growth conditions.** GFP-expressing *Nicotiana benthamiana* line 16c (63) was grown under 100 µmole m^{-2} s^{-1} light in a 16 h photoperiod at 21°C in Snijder Labs Microclima cabinets.

Transient gene expression and mutation analysis in *Nicotiana benthamiana*. *Agrobacterium tumefaciens* strain AGL1 was transformed with Cpf1, Cas9, and GFP-targeting guide RNA binary vectors and selected using 100 µg/ml spectinomycin and 50 µg/ml rifampicin. For each construct, overnight starter cultures in LB medium with antibiotics were used to inoculate 10 ml of medium for overnight incubation at 28°C and 230 rpm. Overnight cultures were then centrifuged, resuspended in infiltration buffer (10 mM MES [pH 5.6], 300 µM acetosyringeone, 10 mM $MgCl_2$) and incubated for 3 hours at room temperature. Cells were adjusted to 1.0 OD_{595}. AsCpf1 and LbCpf1 cultures were mixed 1:1 with their respective guide RNA cultures. Accordingly, the Cas9 culture was adjusted to 0.5 OD_{595}. For guide RNA-only infiltrations, guide RNA cultures were also adjusted to 0.5 OD_{595}. Cells were infiltrated into the underside of 4-6-week-old *Nicotiana benthamiana* line 16c leaves using a 1 ml syringe without a needle. Infiltrated tissue was harvested 3 days post-infiltration. Leaf genomic DNA was extracted using GenElute Plant Genomic DNA MiniPrep Kit (Sigma) and used for PCR amplification of the GFP locus (Table S1). PCR products were two-fold diluted into 1X NEBuffer2 (New England Biolabs) then denatured and re-annealed for heteroduplex formation (95°C, 10 min; 95-85°C at -2°C/s; 85-25°C at -0.3°C/s). Heteroduplexes were supplemented with T7 endonuclease (0.2 U/µl, New England Biolabs) and incubated at 37°C for 1 h. DNA was resolved on a 2% agarose gel with SYBR Safe staining (Invitrogen) and imaged on a UVP BioDoc-It.

***In vitro* synthesis and purification of Cpf1 guide RNAs.** Single-stranded DNA oligonucleotides containing the reverse complement of the guide RNA sequences were annealed in equimolar quantities to a short T7 RNA polymerase priming sequence in 1X T7 transcription buffer (Invitrogen)

(Table S1). *In vitro* transcription was performed in 100 µl reaction volumes containing annealed template DNA (0.1 µg/µl), RNAseOUT (1 U/µl, Invitrogen), 7.5 mM of each rNTP, 30 mM $MgCl_2$, 10 mM DTT, T7 RNA polymerase (2 U/µl, Invitrogen) in 1X T7 transcription buffer (Invitrogen). Reactions were incubated at 37°C overnight (16 h). Post-incubation, TURBO DNAse was added to remove template DNA (0.2U/µl, Ambion) and incubated at 37°C for 15 min, then enzymes inhibited with EDTA (25 mM). RNA was separated and purified from 10% denaturing TBE-UREA polyacrylamide gels as previously described (64) and quantified using a NanoDrop 1000.

Purification of LbCpf1 protein. *E.coli* codon-optimized LbCpf1 bearing an N-terminal MBP-TEV-HIS-NLS tag was a gift from Jin-Soo Kim (Addgene plasmid #79008). Rosetta (DE3) pLysS cells (EMD Millipore) were transformed with this vector and selected on 50 µg/ml carbenicillin and 50 µg/ml chloramphenicol. An overnight starter culture in LB medium with antibiotics was used to inoculate 1 L medium and incubated at 37°C at 110 rpm. When the culture reached 0.6 OD_{600} it was cooled to 16°C for overnight induction (16 h) with IPTG (0.5 M). Cells were harvested and frozen at -80°C until purification. Cells were resuspended in 10 ml extraction buffer 1 (50 mM HEPES pH 7.5, 1 M NaCl, 5 mM $MgCl_2$, 1 mM PMSF, 10% glycerol, 1x EDTA-free Halt protease inhibitor [Thermo Scientific], 1 mg/ml lysozyme) and incubated on ice for 30 min. An equal volume of extraction buffer 2 was added (50 mM HEPES pH 7.5, 1 M NaCl, 5 mM $MgCl_2$, 1 mM PMSF, 10% glycerol, 1x EDTA-free Halt protease inhibitor [Thermo Scientific], 20 mM imidazole, 4 mM β-mercaptoethanol, 500 mM γ-aminobutyric acid). Cell lysate was sonicated using a Soniprep 150 plus, centrifuged (25,000 *g*, 4°C) and the supernatant passed through a syringe filter (0.22 µm). Cobalt resin (HisPur, Thermo Scientific) was equilibrated in a gravity flow column (Econo-Pac, Bio-Rad) using equilibration buffer (50 mM HEPES pH 7.5, 1 M NaCl, 5 mM $MgCl_2$, 10% glycerol, 10 mM imidazole, 250 mM γ-aminobutyric acid). Cell lysate was then applied, washed (50 mM HEPES pH 7.5, 1 M NaCl, 5 mM $MgCl_2$, 10% glycerol, 10 mM imidazole, 2 mM β-mercaptoethanol, 250 mM γ-aminobutyric acid) and eluted (50 mM HEPES pH 7.5, 1 M NaCl, 5 mM $MgCl_2$, 10% glycerol, 250 mM imidazole, 2 mM β-mercaptoethanol, 250 mM γ-aminobutyric acid). Elutions were analyzed by SDS-PAGE. LbCpf1-containing fractions were pooled, concentrated to 200 µl (Vivaspin 30k MWCO, GE Healthcare) and buffer exchanged (Zeba 40k MWCO, Thermo Scientific) into storage buffer (20 mM HEPES pH 7.5, 500 mM NaCl, 5 mM $MgCl_2$, 1% glycerol, 1 mM DTT, 250 mM γ-aminobutyric acid). Protein concentration was measured using Bradford reagent (Sigma). Final concentration was 30 µg/µl. Single-use aliquots were snap-frozen in liquid nitrogen and stored at -80°C.

***In vitro* cleavage assay.** Genomic DNA was extracted from *Chlamydomonas reinhardtii* using GenElute Plant Genomic DNA MiniPrep Kit (Sigma). Target loci were PCR-amplified and purified using MinElute PCR Purification Kit (QIAGEN) (Table S1). Purified LbCpf1 (200 nM) was pre-incubated with guide RNA

(600 nM) in cleavage buffer (1X NEBuffer3 [New England Biolabs], 10 mM DTT, 10 mM $MgCl_2$) at 37°C for 15 min. Target DNA (20nM) was added to a final volume of 20 µl. Reactions were incubated at 37°C for 1 h. Cleavage reactions were purified using MinElute PCR Purification Kit (QIAGEN) then resolved on 2% agarose gels with SYBR Safe staining (Invitrogen) and imaged on a UVP BioDoc-It.

***Chlamydomonas reinhardtii* cultures.** *Chlamydomonas reinhardtii* strains cc-1883 (*cw15*) and cc-2931 were kindly provided by Dr Sinead Collins. Cells were grown on Tris-Acetate-Phosphate (TAP) media (65) supplemented with 1% agar. Stock cultures were supplemented with 4 g/L yeast extract to encourage the growth of contaminants. Cells were grown under constant illumination with cool fluorescent white light (100 µmol photons m^{-1} s^{-1}) at 28°C, and liquid TAP cultures were shaken at 110 rpm.

***Chlamydomonas* transfection.** Cultures were grown to 2 x 10^6 cells/ml and counted using a hemocytometer. For optional pre-treatment of cc-2931, 5 x 10^5 cells were suspended and centrifuged (5 min, 1500 *g*) in Maxx Efficiency™ Transformation Reagent (1 ml) twice, followed by suspension in the same reagent supplemented with sucrose (40 mM). Purified LbCpf1 (100 µg, 0.526 nmol) was pre-incubated at a 1:3 molar ratio with guide RNA (1.578 nmol) at 37°C for 15 minutes to form ribonucleoprotein complexes (RNPs). For transfection, 250 µl cell culture (5 x 10^5 cells) was supplemented with sucrose (40mM) and mixed with pre-incubated RNPs. For template DNA-mediated editing, ssODN (5.26 nmol) was added at a 1:10 molar ratio to LbCpf1 (Table S2). Final volumes were 270-280 µl. Cells were electroporated in 4mm cuvettes (600 V, 50 µF, 200 Ω) using Gene Pulser Xcell™ (Bio-Rad) as suggested by Dr Kwangryul Baek. Immediately after electroporation, 800 µl of TAP with 40 mM sucrose was added. Cells were recovered overnight (24 h) in 5 ml TAP with 40 mM sucrose shaken at 110 rpm then plated using 30% starch as previously described (20). Cells targeted at *FKB12* were plated onto TAP media supplemented with 10 µM rapamycin and grown under 20 µmol photons m^{-1} s^{-1} of constant illumination to limit rapamycin photodegradation. Cells targeted at *CpFTSY*, *CpSRP43* and *PHT7* were plated onto regular TAP media and grown under 100 µmol photons m^{-1} s^{-1} of constant illumination. Cells targeted at *CpFTSY* and *CpSRP43* were screened for green coloration and chlorophyll fluorescence under a blue light transilluminator (Dark Reader, Clare Chemical Research). Cells targeted at *PHT7* were screened for small colonies at 7-9 days after plating. All plate images were taken using a Canon camera (PowerShot G16) and were adjusted for brightness and contrast using GIMP. Cells were counted using OpenCFU (v3.9.0) using default settings (66).

Sequence analysis. Colony PCR was performed using Phire Plant Direct PRC Kit (Thermo Scientific) and appropriate primers (Table S1). To prepare reactions for sequencing, PCR reactions were two-fold diluted, supplemented with exonuclease I (0.18 U/µl, New England Biolabs) and shrimp alkaline phosphatase (0.066 U/µl, New England Biolabs) and incubated at 30°C for 30 min then 80°C for 10 min

for enzyme denaturation. Reactions were sequenced using BigDye Terminator v3.1 (Applied Biosystems) followed by capillary analysis at Edinburgh Genomics. Low quality sequences (typically Q40/length < 0.3), were excluded together with mixed-read sequences. Sequences were aligned using Clustal Omega (67).

Immunoblot. Liquid cell cultures were harvested and snap-frozen in mid-log phase. Cells were suspended in extraction buffer (20 mM Tris-HCl pH 7.5, 5 mM MgCl2, 300 mM NaCl, 5 mM DTT, 0.1% NP40, 1x EDTA-free Halt protease inhibitor [Thermo Scientific]). Total soluble protein was extracted by two freeze/thaw cycles in liquid nitrogen followed by centrifuge at 17000 *g* for 15 min at 4 ^{o}C. The supernatant was measured using Bradford reagent (Sigma). Then, 40 µg total protein was resolved on a 16% Tricine SDS-PAGE gel (68). Running conditions were 30 V for 1 h followed by 50 V for 6 h. The gel was transferred onto a 0.45 µm nitrocellulose membrane using the wet transfer method (30 V for 1 h at 4^{o}C). The membrane was blocked overnight with 5% milk and hybridized using mouse anti-his antibodies [His-Tag (27E8) Mouse mAb #2366, Cell Signaling Technology] and subsequently anti-mouse horseradish peroxidase-linked secondary antibodies (Anti-mouse IgG, HRP-linked Antibody #7076, Cell signaling technology). Peroxidase activity was detected using Pierce ECL substrate (Thermo Scientific) and developed for 1 h.

Acknowledgements

We thank Dr Martin Wear, Dr Sophie Kneeshaw and Dr Cihan Makbul for suggestions in protein purification, Dr Kwangryul Baek for advising on Chlamydomonas electroporation and Prof. Andrew Hudson for critically reading the manuscript. AM is a Chancellor's Fellow at the University of Edinburgh. This work was supported by the BBSRC PHYCONET Proof of Concept Fund, PHYCPoC-31.

References

1. Harris EH (2001) *CHLAMYDOMONAS* AS A MODEL ORGANISM. *Annu Rev Plant Physiol Plant Mol Biol* 52:363-406.
2. Benning C (2015) Fueling research on *Chlamydomonas*. *Plant J* 82(3):363-364.
3. Goodenough U (2015) Historical perspective on *Chlamydomonas* as a model for basic research: 1950-1970. *Plant J* 82(3):365-369.
4. Wang Y, Duanmu D, & Spalding MH (2011) Carbon dioxide concentrating mechanism in *Chlamydomonas reinhardtii*: inorganic carbon transport and CO2 recapture. *Photosynth Res* 109(1-3):115-122.
5. Wang Y, Stessman DJ, & Spalding MH (2015) The CO2 concentrating mechanism and photosynthetic carbon assimilation in limiting CO2 : how *Chlamydomonas* works against the gradient. *Plant J* 82(3):429-448.
6. Silflow CD & Lefebvre PA (2001) Assembly and motility of eukaryotic cilia and flagella. Lessons from *Chlamydomonas reinhardtii*. *Plant Physiol* 127(4):1500-1507.
7. Pazour GJ, Agrin N, Leszyk J, & Witman GB (2005) Proteomic analysis of a eukaryotic cilium. *J Cell Biol* 170(1):103-113.

8. Pazour GJ, Agrin N, Walker BL, & Witman GB (2006) Identification of predicted human outer dynein arm genes: candidates for primary ciliary dyskinesia genes. *J Med Genet* 43(1):62-73.
9. Merchant SS, Kropat J, Liu B, Shaw J, & Warakanont J (2012) TAG, you're it! Chlamydomonas as a reference organism for understanding algal triacylglycerol accumulation. *Curr Opin Biotechnol* 23(3):352-363.
10. Li-Beisson Y, Beisson F, & Riekhof W (2015) Metabolism of acyl-lipids in *Chlamydomonas reinhardtii*. *Plant J* 82(3):504-522.
11. Scranton MA, Ostrand JT, Fields FJ, & Mayfield SP (2015) *Chlamydomonas* as a model for biofuels and bio-products production. *Plant J* 82(3):523-531.
12. Lohr M, Im CS, & Grossman AR (2005) Genome-based examination of chlorophyll and carotenoid biosynthesis in *Chlamydomonas reinhardtii*. *Plant Physiol* 138(1):490-515.
13. Philipps G, Happe T, & Hemschemeier A (2012) Nitrogen deprivation results in photosynthetic hydrogen production in *Chlamydomonas reinhardtii*. *Planta* 235(4):729-745.
14. Boyle NR*, et al.* (2012) Three acyltransferases and nitrogen-responsive regulator are implicated in nitrogen starvation-induced triacylglycerol accumulation in *Chlamydomonas*. *J Biol Chem* 287(19):15811-15825.
15. Juergens MT*, et al.* (2015) The regulation of photosynthetic structure and function during nitrogen deprivation in *Chlamydomonas reinhardtii*. *Plant Physiol* 167(2):558-573.
16. Maul JE*, et al.* (2002) The *Chlamydomonas reinhardtii* plastid chromosome: islands of genes in a sea of repeats. *Plant Cell* 14(11):2659-2679.
17. Merchant SS*, et al.* (2007) The *Chlamydomonas* genome reveals the evolution of key animal and plant functions. *Science* 318(5848):245-250.
18. Kindle KL, Schnell RA, Fernández E, & Lefebvre PA (1989) Stable nuclear transformation of *Chlamydomonas* using the *Chlamydomonas* gene for nitrate reductase. *J Cell Biol* 109(6 Pt 1):2589-2601.
19. Kindle KL (1990) High-frequency nuclear transformation of *Chlamydomonas reinhardtii*. *Proc Natl Acad Sci U S A* 87(3):1228-1232.
20. Shimogawara K, Fujiwara S, Grossman A, & Usuda H (1998) High-efficiency transformation of *Chlamydomonas reinhardtii* by electroporation. *Genetics* 148(4):1821-1828.
21. Kim S*, et al.* (2014) A simple and non-invasive method for nuclear transformation of intact-walled *Chlamydomonas reinhardtii*. *PLoS One* 9(7):e101018.
22. Harris EH, Stern DB, & Witman GB (2009) The Chlamydomonas Sourcebook *(2nd ed.)* (Academic Press, San Diego).
23. Debuchy R, Purton S, & Rochaix JD (1989) The argininosuccinate lyase gene of *Chlamydomonas reinhardtii*: an important tool for nuclear transformation and for correlating the genetic and molecular maps of the ARG7 locus. *EMBO J* 8(10):2803-2809.
24. Sodeinde OA & Kindle KL (1993) Homologous recombination in the nuclear genome of *Chlamydomonas reinhardtii*. *Proc Natl Acad Sci U S A* 90(19):9199-9203.
25. Mayfield SP & Kindle KL (1990) Stable nuclear transformation of *Chlamydomonas reinhardtii* by using a *C. reinhardtii* gene as the selectable marker. *Proc Natl Acad Sci U S A* 87(6):2087-2091.
26. Gumpel NJ, Rochaix JD, & Purton S (1994) Studies on homologous recombination in the green alga *Chlamydomonas reinhardtii*. *Curr Genet* 26(5-6):438-442.
27. Slaninová M, Dominika H, Vlček D, & Mages W (2008) Is it possible to improve homologous recombinationin *Chlamydomonas reinhardtii*? *Biologia* 63(6):941-946.
28. Mages W*, et al.* (2007) Complementation of the *Chlamydomonas reinhardtii* arg7-8 (arg2) point mutation by recombination with a truncated nonfunctional ARG7 gene. *Protist* 158(4):435-446.
29. Zorin B, Hegemann P, & Sizova I (2005) Nuclear-gene targeting by using single-stranded DNA avoids illegitimate DNA integration in *Chlamydomonas reinhardtii*. *Eukaryot Cell* 4(7):1264-1272.

30. Zorin B, Lu Y, Sizova I, & Hegemann P (2009) Nuclear gene targeting in *Chlamydomonas* as exemplified by disruption of the PHOT gene. *Gene* 432(1-2):91-96.
31. Jiang WZ, Dumm S, Knuth ME, Sanders SL, & Weeks DP (2017) Precise oligonucleotide-directed mutagenesis of the *Chlamydomonas reinhardtii* genome. *Plant Cell Rep* 36(6):1001-1004.
32. Greiner A*, et al.* (2017) Targeting of Photoreceptor Genes in *Chlamydomonas* reinhardtii via Zinc-finger Nucleases and CRISPR/Cas9. *Plant Cell*.
33. Sizova I, Greiner A, Awasthi M, Kateriya S, & Hegemann P (2013) Nuclear gene targeting in *Chlamydomonas* using engineered zinc-finger nucleases. *Plant J* 73(5):873-882.
34. Jiang W, Brueggeman AJ, Horken KM, Plucinak TM, & Weeks DP (2014) Successful transient expression of Cas9 and single guide RNA genes in *Chlamydomonas reinhardtii*. *Eukaryot Cell* 13(11):1465-1469.
35. Shin SE*, et al.* (2016) CRISPR/Cas9-induced knockout and knock-in mutations in *Chlamydomonas reinhardtii*. *Sci Rep* 6:27810.
36. Baek K*, et al.* (2016) DNA-free two-gene knockout in *Chlamydomonas reinhardtii* via CRISPR-Cas9 ribonucleoproteins. *Sci Rep* 6:30620.
37. Bae S, Kweon J, Kim HS, & Kim JS (2014) Microhomology-based choice of Cas9 nuclease target sites. *Nat Methods* 11(7):705-706.
38. van Overbeek M*, et al.* (2016) DNA Repair Profiling Reveals Nonrandom Outcomes at Cas9-Mediated Breaks. *Mol Cell* 63(4):633-646.
39. Yoon HS, Hackett JD, Ciniglia C, Pinto G, & Bhattacharya D (2004) A molecular timeline for the origin of photosynthetic eukaryotes. *Mol Biol Evol* 21(5):809-818.
40. Belhaj K, Chaparro-Garcia A, Kamoun S, Patron NJ, & Nekrasov V (2015) Editing plant genomes with CRISPR/Cas9. *Curr Opin Biotechnol* 32:76-84.
41. Zetsche B*, et al.* (2017) Multiplex gene editing by CRISPR-Cpf1 using a single crRNA array. *Nat Biotechnol* 35(1):31-34.
42. Tu M*, et al.* (2017) A 'new lease of life': FnCpf1 possesses DNA cleavage activity for genome editing in human cells. *Nucleic Acids Res*.
43. Xu R*, et al.* (2016) Generation of targeted mutant rice using a CRISPR-Cpf1 system. *Plant Biotechnol J*.
44. Hu X, Wang C, Liu Q, Fu Y, & Wang K (2017) Targeted mutagenesis in rice using CRISPR-Cpf1 system. *J Genet Genomics* 44(1):71-73.
45. Kim H*, et al.* (2017) CRISPR/Cpf1-mediated DNA-free plant genome editing. *Nat Commun* 8:14406.
46. Tang X*, et al.* (2017) A CRISPR-Cpf1 system for efficient genome editing and transcriptional repression in plants. *Nat Plants* 3:17018.
47. Crespo JL, Díaz-Troya S, & Florencio FJ (2005) Inhibition of target of rapamycin signaling by rapamycin in the unicellular green alga *Chlamydomonas reinhardtii*. *Plant Physiol* 139(4):1736-1749.
48. Bae S, Park J, & Kim JS (2014) Cas-OFFinder: a fast and versatile algorithm that searches for potential off-target sites of Cas9 RNA-guided endonucleases. *Bioinformatics* 30(10):1473-1475.
49. Kirst H, García-Cerdán JG, Zurbriggen A, & Melis A (2012) Assembly of the light-harvesting chlorophyll antenna in the green alga *Chlamydomonas reinhardtii* requires expression of the TLA2-CpFTSY gene. *Plant Physiol* 158(2):930-945.
50. Kirst H, Garcia-Cerdan JG, Zurbriggen A, Ruehle T, & Melis A (2012) Truncated photosystem chlorophyll antenna size in the green microalga *Chlamydomonas reinhardtii* upon deletion of the TLA3-CpSRP43 gene. *Plant Physiol* 160(4):2251-2260.
51. Bothmer A*, et al.* (2017) Characterization of the interplay between DNA repair and CRISPR/Cas9-induced DNA lesions at an endogenous locus. *Nat Commun* 8:13905.

52. Richardson CD*, et al.* (2017) CRISPR-Cas9 genome editing in human cells works via the Fanconi Anemia pathway. *bioRxiv* 10.1101/136028.
53. Zhang R*, et al.* (2014) High-Throughput Genotyping of Green Algal Mutants Reveals Random Distribution of Mutagenic Insertion Sites and Endonucleolytic Cleavage of Transforming DNA. *Plant Cell* 26(4):1398-1409.
54. Kim HK*, et al.* (2017) In vivo high-throughput profiling of CRISPR-Cpf1 activity. *Nat Methods* 14(2):153-159.
55. Doench JG*, et al.* (2014) Rational design of highly active sgRNAs for CRISPR-Cas9-mediated gene inactivation. *Nat Biotechnol* 32(12):1262-1267.
56. Chari R, Mali P, Moosburner M, & Church GM (2015) Unraveling CRISPR-Cas9 genome engineering parameters via a library-on-library approach. *Nat Methods* 12(9):823-826.
57. Xu H*, et al.* (2015) Sequence determinants of improved CRISPR sgRNA design. *Genome Res* 25(8):1147-1157.
58. Doench JG*, et al.* (2016) Optimized sgRNA design to maximize activity and minimize off-target effects of CRISPR-Cas9. *Nat Biotechnol* 34(2):184-191.
59. Hough SH, Ajetunmobi A, Brody L, Humphryes-Kirilov N, & Perello E (2016) Desktop Genetics. *Per Med* 13(6):517-521.
60. Chen F*, et al.* (2017) Targeted activation of diverse CRISPR-Cas systems for mammalian genome editing via proximal CRISPR targeting. *Nat Commun* 8:14958.
61. Yamano T, Iguchi H, & Fukuzawa H (2013) Rapid transformation of *Chlamydomonas reinhardtii* without cell-wall removal. *J Biosci Bioeng* 115(6):691-694.
62. Fauser F, Schiml S, & Puchta H (2014) Both CRISPR/Cas-based nucleases and nickases can be used efficiently for genome engineering in *Arabidopsis thaliana*. *The Plant journal : for cell and molecular biology* 79(2):348-359.
63. Ruiz MT, Voinnet O, & Baulcombe DC (1998) Initiation and maintenance of virus-induced gene silencing. *Plant Cell* 10(6):937-946.
64. Harris CJ, Molnar A, Muller SY, & Baulcombe DC (2015) FDF-PAGE: a powerful technique revealing previously undetected small RNAs sequestered by complementary transcripts. *Nucleic acids research* 43(15):7590-7599.
65. Gorman DS & Levine RP (1965) Cytochrome f and plastocyanin: their sequence in the photosynthetic electron transport chain of *Chlamydomonas reinhardi*. *Proc Natl Acad Sci U S A* 54(6):1665-1669.
66. Geissmann Q (2013) OpenCFU, a new free and open-source software to count cell colonies and other circular objects. *PLoS One* 8(2):e54072.
67. Li W*, et al.* (2015) The EMBL-EBI bioinformatics web and programmatic tools framework. *Nucleic Acids Res* 43(W1):W580-584.
68. Schägger H (2006) Tricine-SDS-PAGE. *Nat Protoc* 1(1):16-22.

Figure Legends

Fig. 1. Cpf1 activity *in planta* and *in vitro*. (*A*) CRISPR nuclease orthologues *Acidaminococcus sp.* Cpf1 (AsCpf1), *Lachnospiraceae bacterium* Cpf1 (LbCpf1) and *Streptococcus pyogenes* Cas9 (SpCas9) were expressed *in planta* with corresponding guide RNAs (gRNAs) targeting the GFP locus in *Nicotiana benthamiana* line 16c. T7 mismatch endonuclease digestion of the PCR-amplified GFP locus from a mixed-population of cells results in cleaved products (black arrows), corresponding to edited DNA. L: ladder. (*B*) *In vitro* cleavage of PCR-amplified *FKB12* using LbCpf1 and gRNA ribonucleoproteins (RNP). Arrowheads indicate cleaved products. L: ladder. (*C*) Sequencing of cells edited at *FKB12* using LbCpf1

RNPs. *FKB12* was amplified from rapamycin-resistant colonies growing on solid growth media with 10 µM rapamycin (n=16). Black triangles indicate the expected LbCpf1-mediated cleavage site, red triangles indicate insertion sites with insertion lengths shown to the right of the sequence, red highlighting indicates sequence deviation from the wild-type (wt) sequence (top).

Fig. 2. Co-delivery of LbCpf1 and gRNA ribonucleoproteins (RNPs) and single-stranded oligodeoxynucleotides (ssODNs) into *C. reinhardtii*. (*A*) Schematic of sense or antisense ssODN-mediated DNA repair upon co-delivery of RNPs and ssODNs. (*B*) Cells co-transfected with RNPs and sense or antisense ssODNs were serially diluted and each dilution spread onto solid growth media with and without rapamycin (rap, 10 µM). A dilution with countable numbers of colonies (n) is shown for each treatment and the percentage of rapamycin resistant colonies indicated. (*C*) Representative sequences of rapamycin-resistant colonies from the 'LbCpf1 + sense ssODN' experiment. All sequence deviations from the expected knock-in (top) and wild type (wt) sequences (bottom) within the span of the ssODN homology region are shown. Sequence highlighting is as in Fig. 1*C*. Stop codons are underlined in red. Sequences from all resistant colonies are collated in Fig. S2 and Fig. S3.

Fig. 3. Selection-free identification of his-tagged *FKB12* mutants. (*A*) Schematic of the his-tagged *FKB12* locus obtained using sense ssODNs carrying an in-frame his_6-tag followed by a stop codon. (*B*) Cells co-transfected with RNPs and ssODNs plated as described in Fig. 2*B*. (*C*) *FKB12* sequences of six rapamycin-resistant colonies from the plate with rapamycin shown in panel B, three of which carry scarless, ssODN-mediated editing. (*D*) *FKB12* sequences from 13 colonies randomly chosen from the plate without rapamycin in panel B, one of which carries scarless, ssODN-mediated editing. All sequence deviations from the expected knock-in (top) and wild type (wt) sequences (bottom) within the span of the ssODN homology region are shown. Sequence highlighting is as in Fig. 1*C* and Fig. 2*C*. (*E*) Immunoblot analysis of the four scarless, sequenced mutants (labelled 1-4) shown in panels C and D.

Fig. 4. Targeting of *CpFTSY*, *CpSRP43* and *PHT7* using RNPs and sense ssODNs. (*A*) *In vitro* cleavage of *CpFTSY*, *CpSRP43*, and *PHT7*. Arrowheads indicate cleaved products, asterisk denotes a non-specific band. L: ladder. (*B*) Representative plates of the bright-green phenotype of *CpFTSY* and *CpSRP43* mutants and the slow-growth phenotype of *PHT7* mutants (arrowheads). Indicated colonies are enlarged (bottom right panels) alongside a colony from each plate which was not identified through screening and is thus take to represent wild-type (wt) (*C*) Sequences from all cells identified as tentative *CpFTSY* (top), *CpSRP43* (middle) and *PHT7* (bottom) mutants through phenotypic selection. Images of all screened plates and selected cells are in Fig. S5*B* and Fig. S6. All sequence deviations from the expected knock-in (top) and wild-type (wt) sequences (bottom) within the span of the ssODN homology region are shown. Sequence highlighting is as in Fig. 1*C*, Fig. 2*C* and Fig. 3*D*. (*D*) Numbers of

screened colonies and sequence verified mutants identified in cells edited at *CpFTSY*, *CpSRP43* and *PHT7*. Colony numbers as a proportion of all screened colonies are shown in parentheses. One tentative *CpFTSY* mutant grew as a mixed colony and could not be isolated (asterisk, Fig. S6).

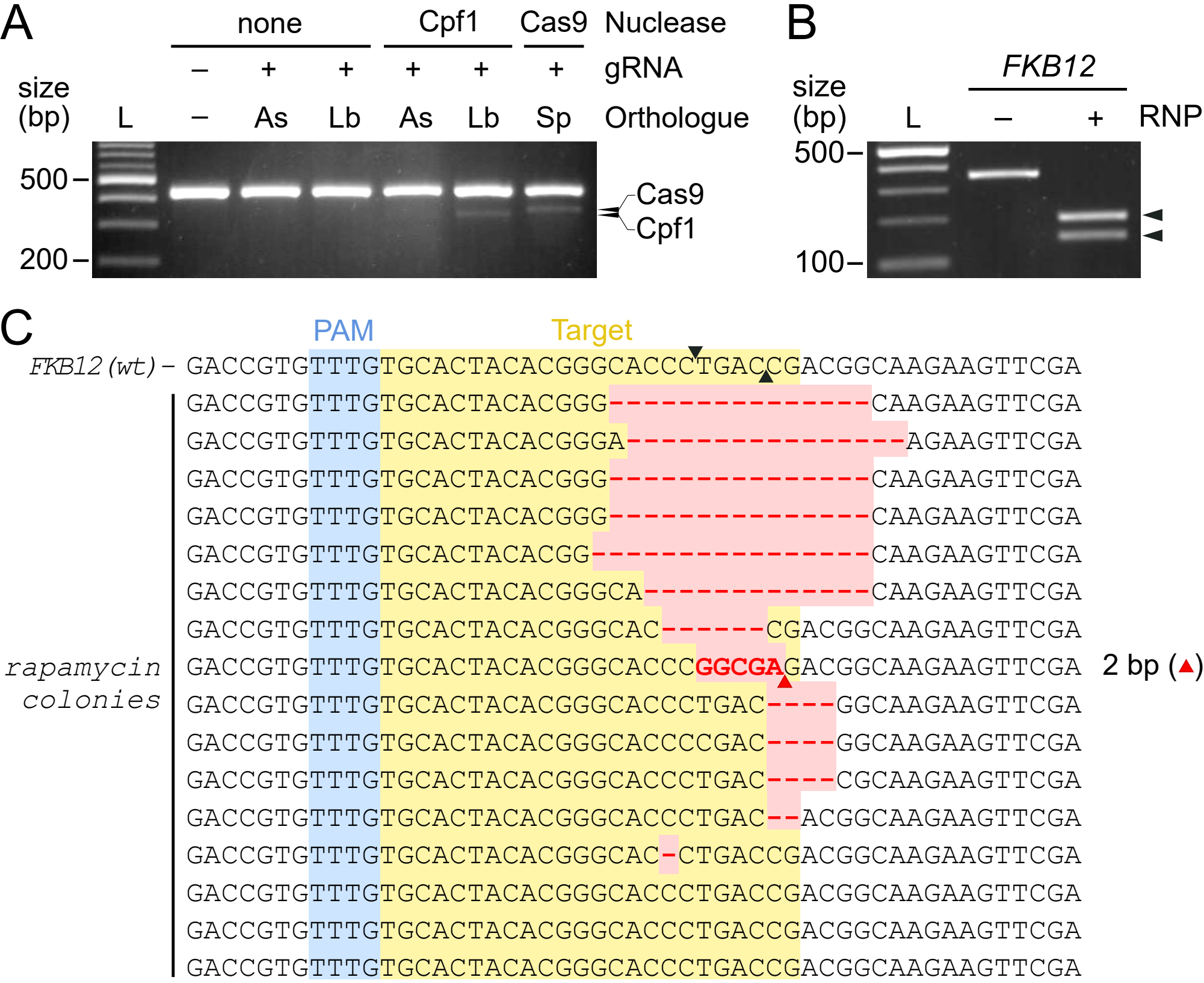
A
none
Cpf1
Cas9
Nuclease
–
+
+
+
+
+
gRNA
size
(bp)
L
–
As
Lb
As
Lb
Sp
Orthologue
500
200
Cas9
Cpf1
B
FKB12
size
(bp)
L
–
+
RNP
500
100
C
PAM
Target
FKB12(wt) – GACCGTGTTTGTGCACTACACGGGCACCCTGACCGACGGCAAGAAGTTCGA
GACCGTGTTTGTGCACTACACGGG----------CAAGAAGTTCGA
GACCGTGTTTGTGCACTACACGGGA----------AGAAGTTCGA
GACCGTGTTTGTGCACTACACGGG----------CAAGAAGTTCGA
GACCGTGTTTGTGCACTACACGGG----------CAAGAAGTTCGA
GACCGTGTTTGTGCACTACACGG----------CAAGAAGTTCGA
GACCGTGTTTGTGCACTACACGGGCA----------CAAGAAGTTCGA
GACCGTGTTTGTGCACTACACGGGCAC------CGACGGCAAGAAGTTCGA
rapamycin colonies
GACCGTGTTTGTGCACTACACGGGCACCCGGCGAGACGGCAAGAAGTTCGA
2 bp (▲)
GACCGTGTTTGTGCACTACACGGGCACCCTGAC----GGCAAGAAGTTCGA
GACCGTGTTTGTGCACTACACGGGCACCCCGAC----GGCAAGAAGTTCGA
GACCGTGTTTGTGCACTACACGGGCACCCTGAC----CGCAAGAAGTTCGA
GACCGTGTTTGTGCACTACACGGGCACCCTGAC--ACGGCAAGAAGTTCGA
GACCGTGTTTGTGCACTACACGGGCAC-CTGACCGACGGCAAGAAGTTCGA
GACCGTGTTTGTGCACTACACGGGCACCCTGACCGACGGCAAGAAGTTCGA
GACCGTGTTTGTGCACTACACGGGCACCCTGACCGACGGCAAGAAGTTCGA
GACCGTGTTTGTGCACTACACGGGCACCCTGACCGACGGCAAGAAGTTCGA

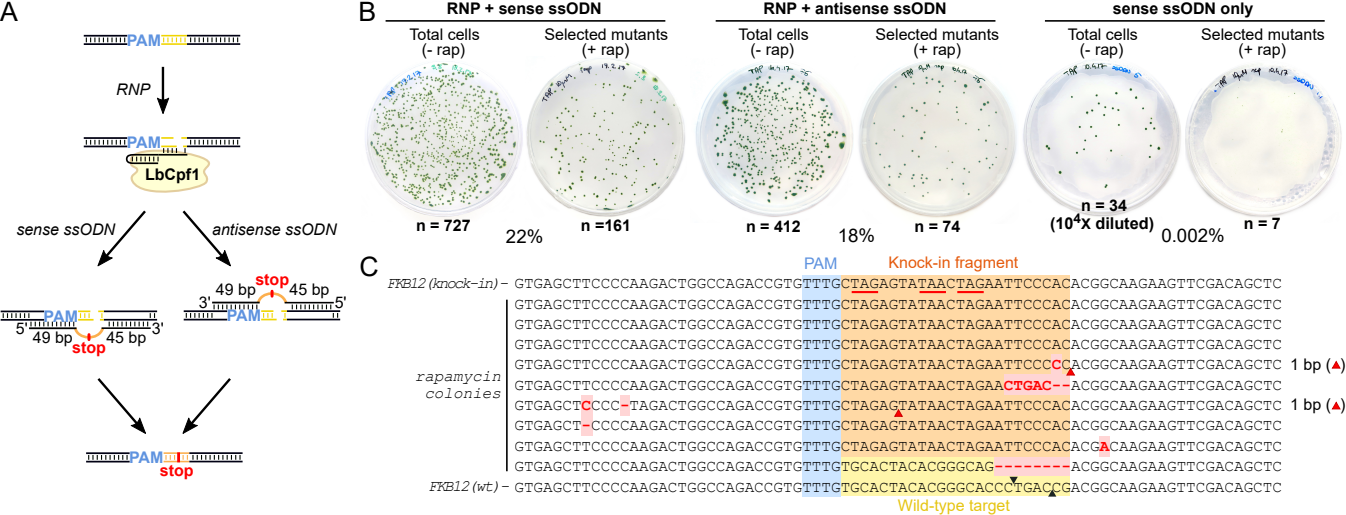
A
PAM
RNP
PAM
LbCpf1
sense ssODN
antisense ssODN
5'
PAM
3'
49 bp
stop
45 bp
3'
PAM
5'
49 bp
stop
45 bp
PAM
stop
B
RNP + sense ssODN
Total cells (- rap)
Selected mutants (+ rap)
n = 727
22%
n =161
RNP + antisense ssODN
Total cells (- rap)
Selected mutants (+ rap)
n = 412
18%
n = 74
sense ssODN only
Total cells (- rap)
Selected mutants (+ rap)
n = 34 (10^4X diluted)
0.002%
n = 7
C
PAM
Knock-in fragment
FKB12 (knock-in) - GTGAGCTTCCCCAAGACTGGCCAGACCGTGTTTGCTAGAGTATAACTAGAATTCCCACACGGCAAGAAGTTCGACAGCTC
rapamycin colonies
GTGAGCTTCCCCAAGACTGGCCAGACCGTGTTTGCTAGAGTATAACTAGAATTCCCACACGGCAAGAAGTTCGACAGCTC
GTGAGCTTCCCCAAGACTGGCCAGACCGTGTTTGCTAGAGTATAACTAGAATTCCCACACGGCAAGAAGTTCGACAGCTC
GTGAGCTTCCCCAAGACTGGCCAGACCGTGTTTGCTAGAGTATAACTAGAATTCCCACACGGCAAGAAGTTCGACAGCTC
GTGAGCTTCCCCAAGACTGGCCAGACCGTGTTTGCTAGAGTATAACTAGAATTCCCCCACGGCAAGAAGTTCGACAGCTC 1 bp (▲)
GTGAGCTTCCCCAAGACTGGCCAGACCGTGTTTGCTAGAGTATAACTAGAACTGAC--ACGGCAAGAAGTTCGACAGCTC
GTGAGCTCCCC-TAGACTGGCCAGACCGTGTTTGCTAGAGTATAACTAGAATTCCCACACGGCAAGAAGTTCGACAGCTC 1 bp (▲)
GTGAGCT-CCCCAAGACTGGCCAGACCGTGTTTGCTAGAGTATAACTAGAATTCCCACACGGCAAGAAGTTCGACAGCTC
GTGAGCTTCCCCAAGACTGGCCAGACCGTGTTTGCTAGAGTATAACTAGAATTCCCACACGACAAGAAGTTCGACAGCTC
GTGAGCTTCCCCAAGACTGGCCAGACCGTGTTTGTGCACTACACGGGCAG--------ACGGCAAGAAGTTCGACAGCTC
FKB12 (wt) - GTGAGCTTCCCCAAGACTGGCCAGACCGTGTTTGTGCACTACACGGGCACCCTGACCGACGGCAAGAAGTTCGACAGCTC
Wild-type target

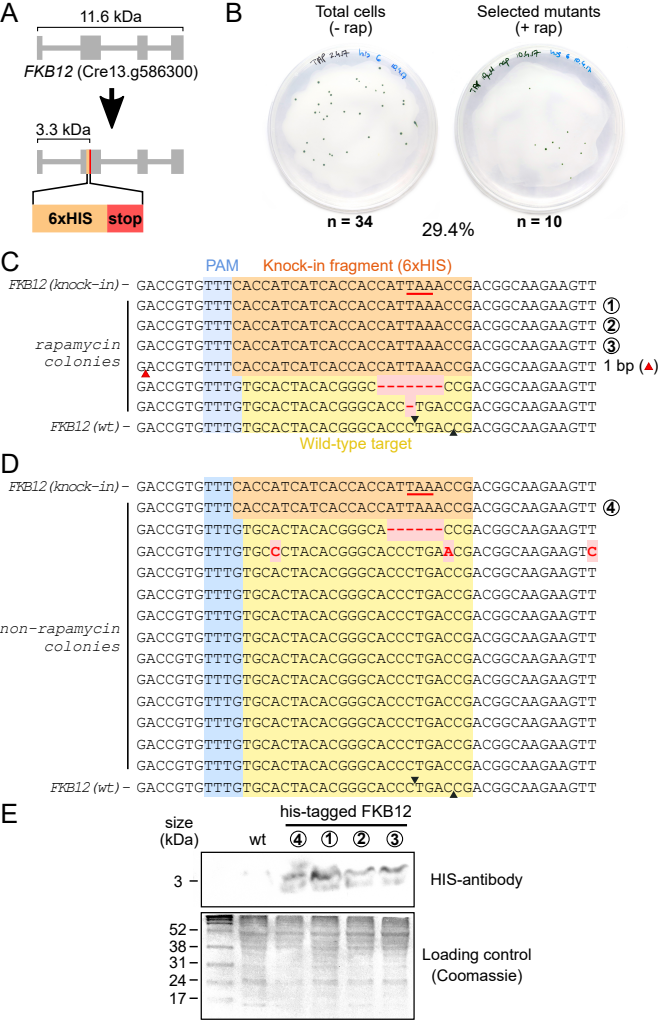
A
11.6 kDa
FKB12 (Cre13.g586300)
3.3 kDa
6xHIS
stop
B
Total cells
(- rap)
Selected mutants
(+ rap)
n = 34
29.4%
n = 10
C
PAM
Knock-in fragment (6xHIS)
FKB12 (knock-in) -
rapamycin
colonies
1 bp (▲)
FKB12 (wt) -
Wild-type target
D
FKB12 (knock-in) -
non-rapamycin
colonies
FKB12 (wt) -
E
size
(kDa)
wt
his-tagged FKB12
3 -
HIS-antibody
52 -
38 -
31 -
24 -
17 -
Loading control
(Coomassie)

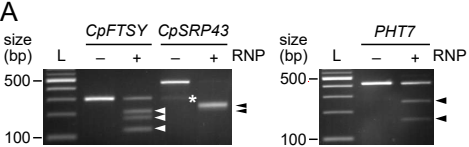

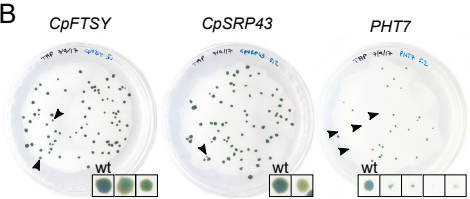

D

	CpFTSY	*CpSRP43*	*PHT7*
Screened colonies	797	810	61
Selected colonies	5*	3	12
Mutants	4 (0.50%)	3 (0.37%)	10 (16.4%)
Knock-in mutants	4 (0.50%)	3 (0.37%)	8 (13.1%)
Scarless mutants	2 (0.25%)	1 (0.12%)	4 (8.2%)